SCATTERING BY SURFACE-BREAKING AND SUB-SURFACE CRACKS

J.D. Achenbach, R.J. Brind and A. Norris
The Technological Institute
Northwestern University
Evanston, IL. 60201

ABSTRACT

This paper is concerned with exact solutions and approximate solutions in the high-frequency domain for scattering of time-harmonic waves by surface-breaking cracks and cracks which are located near a free surface. Both incident surface waves and incident body waves have been considered. The high-frequency approximate solutions are generally based on elastodynamic ray theory. Some approximate solutions based on the Kirchhoff approximation have been included for comparison.

INTRODUCTION

Elastodynamic ray theory provides a powerful tool for the computation of fields generated by scattering of time-harmonic waves by cracks, when the wavelengths of the incident wave is of the same order of magnitude as characteristic length parameters of the crack. Ray theory has the advantage of simplicity and intuitive appeal. The rules that govern reflection, refraction, and edge diffraction of rays are well established, and it is generally not difficult to trace rays from a source via the scatterer to an observer. Fourier methods can be used to relate pulses in the time domain to spectra in the frequency domain.

Experimental setups generally include instrumentation to gate out the relevant pulses in the scattered field on the basis of arrival times. The application of a Fast Fourier Transform to these pulses subsequently yields frequency spectra. In the frequency domain the raw scattering data can conveniently be corrected for transducer transfer functions and other characteristics of the system, which have been obtained on the basis of appropriate calibrations. The corrected amplitudes and phase functions can then be compared with theoretical results that have been obtained by harmonic analysis. For short pulses the frequency spectra of the diffracted signals are centered in the high-frequency (short wavelength) range. Ray theory gives excellent results at such high frequencies.

High-frequency incident waves give rise to interference phenomena which can often easily be interpreted on the basis of ray tracing, and which can provide the basis for an inversion procedure. Particularly the first arriving signals, which are related to the longitudinal waves in the solid, often give rise to a simple structure in the frequency domain.

Considerable progress has been achieved in recent years in the application of elastodynamic ray theory to scattering by cracks. For cracks in unbounded solids theoretical results have been given by Achenbach et al [1]-[4]. For two-dimensional problems ray theory results have been compared with exact results in Ref.[5], and with experimental results in Ref.[6].

In this paper we consider surface-breaking cracks and cracks in the immediate vicinity of a boundary. We start with a brief discussion of exact solutions. For the surface breaking crack we briefly discuss the application of ray theory. For the sub-surface crack approximations to the scattered field are obtained both by ray theory and by the Kirchhoff approximation. We also discuss some pulse-echo computations for the case that the transducer is near the zone of specular reflection from a surface-breaking crack.

2. SURFACE-BREAKING CRACKS

The surface breaking crack is one of the most harmful crack configurations, and it is thus not surprising that there is a considerable interest in their detection. In this section we review solutions to the direct scattering problem for incident surface waves and incident bulk waves. The geometry is shown in Fig. 1.

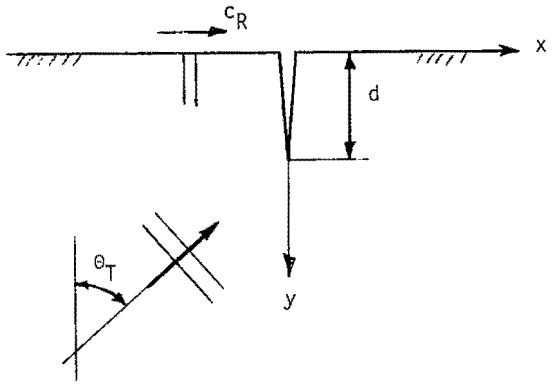

Fig. 1 Surface-breaking crack in an elastic solid.

2.1 Incident waves of anti-plane strain. With reference to the coordinate system shown in Fig. 1, waves of anti-plane strain are defined by displacements in the z-direction which are functions of x and y only. These displacement components, w(x,y) satisfy the reduced wave equation

$$\nabla^2 w + k_T^2 w = 0 . \qquad (2.1)$$

In Eq.(2.1), ∇^2 is the two-dimensional Laplacian and $k_T = \omega/c_T$, where ω is the circular frequency and c_T is the velocity of transverse waves. Here it is implied that the waves are time-harmonic, but the term $\exp(-i\omega t)$ has been omitted, as it will be in the sequel. The boundary conditions are

$$y = 0, \; -\infty < x < \infty: \quad \frac{\partial w}{\partial y} = 0 \qquad (2.2)$$

$$x = 0, \; 0 \le y < d: \quad \frac{\partial w}{\partial x} = 0 . \qquad (2.3)$$

An incident wave of anti-plane strain can be expressed in the form

$$w^i(x,y) = A \exp[ik_T(x\sin\theta_T - y\cos\theta_T)] \qquad (2.4)$$

where $(\sin\theta_T, \cos\theta_T)$ defines the propagation direction. In the absence of the surface breaking crack, the incident wave would give rise to a reflected wave of the form

$$w^r(x,y) = A \exp[ik_T(x\sin\theta_T + y\cos\theta_T)] . \qquad (2.5)$$

It is easily checked that the following condition is satisfied

$$\lim_{y\to 0} \frac{\partial}{\partial y} [w^i(x,y) + w^r(x,y)] = 0 . \qquad (2.6)$$

The total field generated by the interaction of the incident wave (2.4) and the reflected wave (2.5) with the crack, can be expressed by

$$w^t(x,y) = w^i(x,y) + w^r(x,y) + w^s(x,y) \qquad (2.7)$$

where $w^s(x,y)$ is the scattered wave. According to (2.2), $\partial w^t/\partial y$ vanishes at $y = 0$: Equations (2.6) and (2.7) then imply that the boundary condition on the scattered field is

$$\frac{\partial w^s}{\partial y} = 0 , \quad y = 0, \; -\infty < x < \infty . \qquad (2.8)$$

It follows from (2.3)-(2.5) and (2.7) that the scattered field must satisfy the following condition on the crack faces

$$\frac{\partial w^s}{\partial x} = -2iAk_T\sin\theta_T\cos(ik y\cos\theta_T), \quad x = 0^{\pm}, \; 0 \le y \le d . \qquad (2.9)$$

The problem defined by Eqs.(2.1), (2.8) and (2.9) has been solved as a specific and separate problem by Stone et al [7] and Datta [8]. An easier way to obtain a solution can be based on the observation that for anti-plane strain the solution to the surface-breaking crack can be obtained directly from the solution for a crack of length 2d in full space by symmetry considerations. The geometry for this case is shown in Fig. 2.

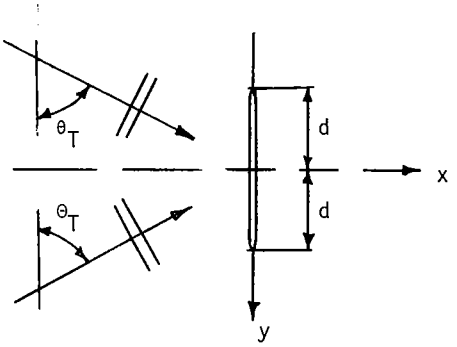

Fig. 2 Crack in unbounded medium with symmetric system of incident waves.

The two incident waves can now be represented by (2.4) and (2.5), and hence (2.6) holds. The scattered field is again defined by (2.7), and the conditions on the crack faces is given by (2.9), except that this condition is now defined over the interior crack of length 2d. Because of the symmetry with respect to y of the right-hand side of (2.9), $w^s(x,y)$ will be symmetric with respect to y, and hence (2.8) will be satisfied automatically.

The high-frequency scattered field for the interior crack can be found in books on acoustics, see, e.g., Ref.[9].

2.2 Incident waves of in-plane strain. Unfortunately, the simple symmetry considerations that hold for the case of anti-plane strain are not valid for the in-plane case. Symmetry considerations do not work because of mode coupling of longitudinal and transverse waves at a traction-free plane. Thus, it is not possible to construct a system of incident waves in an infinite solid with an interior crack, so that the conditions for a surface-breaking crack are automatically satisfied. Hence the problem of scattering by a surface-breaking crack must be considered as a completely separate problem.

Exact solutions for the two-dimensional geometry of a crack of depth d in an elastic half-plane were given in Refs. [10] and [11]. In Ref.[11] the scattered displacement fields due to either a time-harmonic surface wave or a plane time-harmonic longitudinal or transverse body wave incident upon the crack from infinity are investigated. The total field in the half-plane is taken as the superposition of the specified incident field in the uncracked half-plane and the scattered field in the cracked half-plane generated by suitable surface tractions on the crack faces. These tractions are equal and opposite to the tractions generated by the incident wave in the uncracked half-plane when evaluated in the plane of the crack. By decomposing the scattered field into symmetric and anti-symmetric fields with respect to the plane of the crack, a pair of boundary value problems for the quarter-plane is obtained. These two boundary value problems are reduced by integral transform techniques to two uncoupled singular integral equations, which are solved numerically using a collocation scheme. The derivation of the symmetric equation has been presented in Ref.[10], and the derivation of the anti-symmetric integral equation is presented in

Ref.[11]. The crack-opening displacements are then easily calculated from the solutions of the singular integral equations. The exact representations of the diffracted displacement fields are subsequently obtained in the form of finite integrals over the crack length, which are evaluated numerically.

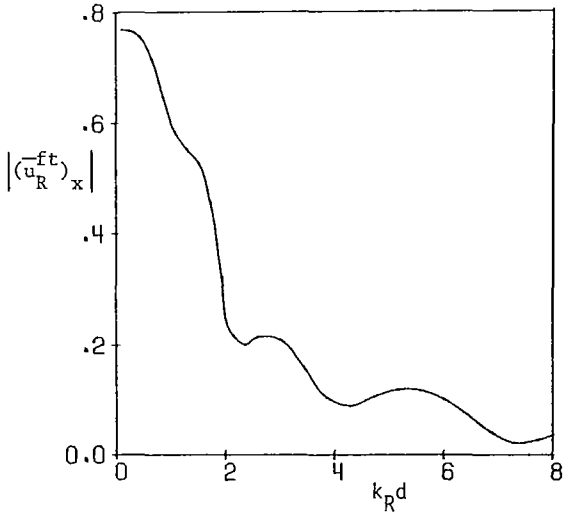

Fig. 3 The total field ahead of the crack (forward-transmitted field)

For an incident Rayleigh wave, Fig. 3 shows the forward-transmitted field, and the back-scattered field is shown in Fig. 4. Apparently, most of the incident wave is backscattered.

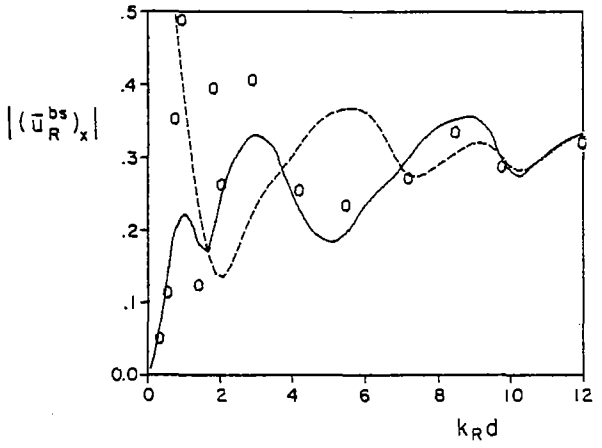

Fig. 4 Comparison of exact and approximate dimensionless x-components of the displacement fields for back-scattered surface waves, where $|(\bar{u}_R^{bs})_x| = |(u_R^{bs})_x| / A(2c_T^2/c_R^2 - 1)$. --- Ray theory of Ref.[12]. O-Exact, see [11]. ——— Asymptotic evaluation of exact integrals of [11].

2.3 Ray Analysis of Surface-Wave Interaction with an Edge Crack In Ref.[12] a simple approximate approach to scattering of Rayleigh surface waves by surface-breaking cracks has been presented, which is valid in the high-frequency range. Solutions are shown to agree well with the results of [11] for $\omega d/c_R > 6$ (see Fig. 4) where ω is the circular frequency, d is the depth of the crack, and c_R is the velocity of Rayleigh surface waves. The method of analysis which is based on elastodynamic ray theory can potentially be extended to scattering by surface-breaking cracks in three-dimensional configurations. The simple concepts of ray tracing that are used suggest simple interpretations of scattering data for the solution of the inverse problem.

An incident Rayleigh wave, propagating in the positive x-direction (see Fig. 1), interacts with the crack. Both the mouth and the edge of the crack act as centers of diffraction, which generate diffracted body waves, and reflected, and transmitted Rayleigh surface waves. The diffracted body waves are neglected but the reflected, transmitted, and diffracted Rayleigh waves are taken into account. The reflections, transmissions, and edge-diffractions are investigated one by one on the basis of elastodynamic ray theory, and the results are then superimposed to yield simple expressions for the back-scattered and forward-scattered Rayleigh surface waves and for the elastodynamic stress-intensity factors, in terms of reflection, transmission, and diffraction coefficients. A simple formula for the inverse problem is presented, which relates the periodicity of the amplitude modulation in the high-frequency range directly to the depth d of the crack.

2.4 Ray analysis of body-wave interaction with an edge crack. Ray theory can conveniently be used to analyze the interaction of in-plane body-waves with a surface-breaking crack. For very short times after the arrival of the first signal, which comes directly from the crack tip, only a few ray-paths need to be considered. Three ray paths are shown in Fig. 5, for an angle of incidence of 60^0, and an angle of observation of 45^0. The incident wave is a longitudinal (L) wave. Since the direction of observation is not near a shadow boundary, or near a boundary of a zone of reflected waves, there are no difficulties with the application of ray theory. In the next section we discuss a case of backscattering for the case that both the angle of incidence and the angle of observation are near 45^0. Then the observation point is near a boundary of a beam of reflected waves, and ray theory cannot be applied in its simplest form.

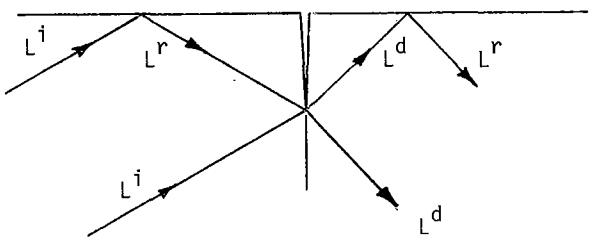

Fig. 5 Three ray paths for incident L-rays

Incident, reflected and diffracted L-rays are denoted by L^i, L^r, and L^d respectively. In Fig.6 we show the following ray paths: L^iL^d, $L^iL^rL^d$, and $L^iL^dL^r$. In the time domain, these ray-paths correspond to the first arrivals. Ray-paths which involve mode conversion (L to T) at the free surface or at the illuminated face of the crack, correspond to later arrivals. In Fig. 6 we have shown the interference of the time-harmonic signals carried by the diffracted L-rays. The figure shows the amplitude modulation for the first two rays (L^iL^d and $L^iL^rL^d$) and for all three rays. The L^iL^d and $L^iL^rL^d$ interference gives rise to a simple pattern in which the crack depth d is related to the spacing of the peaks. The interference of the three rays (L^iL^d, $L^iL^rL^d$ and $L^iL^dL^r$) already produces an amplitude modulation that is not open to immediate interpretation.

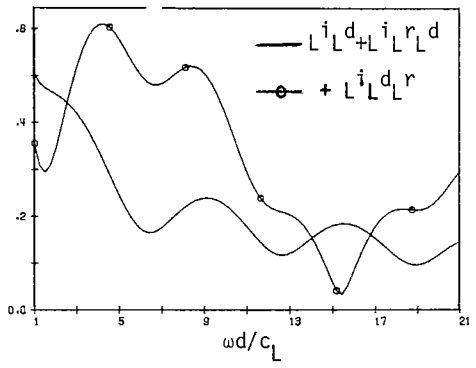

Fig. 6 Amplitudes of diffracted L-rays

2.5 Interference of corner reflection and edge diffraction. When an L-wave transducer is aimed at a surface-breaking crack such that the waves are reflected back from the corner at the crack mouth to the transducer, then under certain circumstances it is observed that the backscattered signal is composed of two distinct parts. These distinct signals in the time domain are thought to be due to reflection from the crack corner and the diffraction from the crack tip. As the transducer is moved slightly, the relative amplitudes of the two signals changes dramatically. In Ref.[13] it has been attempted to estimate the relative amplitudes of the two effects in a high frequency, far field, two dimensional approximation. By high frequency we mean that $k_L d >> 1$, by far field that $d/r >> 1$, where r is the distance from transducer to crack-tip. For a two dimensional approximation we assume a line source behavior for the transducer. Implicit in this two dimensional model is that the crack width is much larger than the transducer width.

The geometry, which corresponds to an experimental set-up, is shown in Fig. 7. The surface-breaking crack of length d is normal to the free surface I at a distance b from a vertex of interior angle ϕ, $0 < \phi < \pi/2$. The transducer is free to be shifted along the free surface II. For any

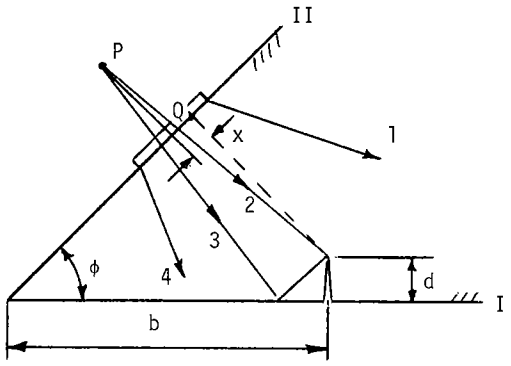

Fig. 7 Surface-breaking crack and location of transducer

positioning of the transducer we define its position as x, where x is the distance of the center of the transducer from Q, the intersection of II and the normal from II to the crack mouth. The distance x is defined as positive in the direction away from the vertex, so for example, in Fig. 7 $x < 0$. The transducer virtual source is at P. A beam of half angle θ_o emanates from P. Each ray of the beam has an associated angle $\theta E[-\theta_o, \theta_o]$, where θ is measured clockwise from the central ray.

As the beam proceeds from P, some of its rays will interact with the crack to produce a scattered signal which may be detected by the transducer. In Fig. 7 the rays 1 and 4 do not interact with the crack. Ray 2 is diffracted by the crack tip to produce a cylindrical wave emanating from the tip. The beam between rays 2 and 3 is both reflected from surface I and scattered from the crack surface. The resultant beam is directed back towards the transducer, where it is detected as a signal with a different phase and amplitude than the purely diffracted signal.

The complete analysis of the diffracted and reflected signals is complicated. Since the transducer is located near a boundary of the zone of reflected waves, ray theory cannot be applied directly. A more sophisticated theory, which is called uniform asymptotic theory, and which includes Fresnel corrections, must be used. Details of the application of such a theory to the problem described above, are given in Ref.[13].

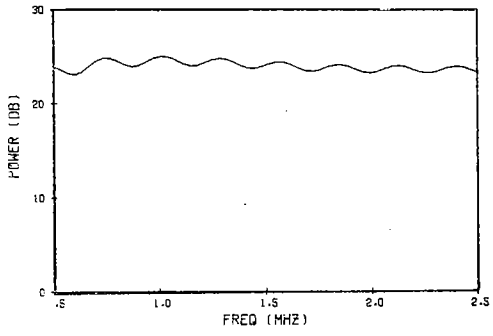

Fig. 8 Power spectrum when the transducer is inside the zone of reflected waves

Figures 8 and 9 show some results. In Fig. 8 the reflected signals from the corner at the crack mouth dominate the diffracted signal from the crack tip. The power spectrum of Fig. 9 is for the case that the reflected and diffracted signals are of the same order of magnitude. This means that the transducer is at the boundary of the zone of reflected waves.

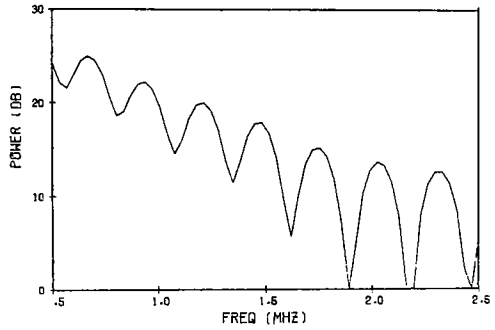

Fig. 9 Power spectrum when the transducer is at the boundary of the zone of reflected waves.

The two curves have been normalized so that they have the same maximum values. Clearly Fig. 9 has a more distinctive character, with a sequency of peaks whose spacing is related to the crack depth d. Figures 8 and 9 show that a slight shift of the transducer transforms the power spectrum from a rather even curve into one with a strong pattern of peaks and valleys, albeit with much smaller actual values of the power.

3. SUB-SURFACE CRACKS

In this Section we summarize some recent results for scattering by a sub-surface crack.

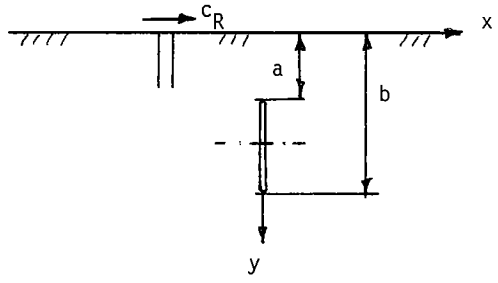

Fig. 10 Geometry for the sub-surface crack

3.1 Scattering of surface waves-exact analysis. In Ref.[14] an exact mathematical analysis has been presented for the scattering of Rayleigh waves by a sub-surface crack. The two-dimensional geometry considered in Ref.[14] is shown in Fig. 10. In Ref.[14] the boundary-value problem for the scattered field is stated, and reduced to an uncoupled system of integral equations, which have been solved numerically. At large distances from the crack the scattered field was shown to consist of outgoing Rayleigh waves and cylindrical body waves.

The integral equations derived in Ref.[14] are of the general form

$$-\sigma^i_{xx} = \frac{\mu}{k_T^2}\int_a^b d_x(y)\, \Gamma_{xx;xx}(0,y;0,y')dy \qquad (3.1)$$

$$-\sigma^i_{xy} = \frac{\mu}{k_T^2}\int_a^b d_y(y)\, \Gamma_{xy;xy}(0,y;0,y')dy \qquad (3.2)$$

together with the side conditions

$$\int_a^b d_i(y)dy = 0\ , \qquad i = x,y\ . \qquad (3.3)$$

$D_i(y) = d_i(y)(b-y)^{1/2}(a-y)^{1/2}$ is continuous in [a,b]. Equations (3.1) and (3.2) must be solved for the density functions $d_i(y)$, i = x,y. In (3.1) and (3.2) σ^i_{xx} and σ^i_{xy} are the stresses due to the incident wave at the location of the crack. The kernels $\Gamma_{xx;xx}$ and $\Gamma_{xy;xy}$ are given by (3.8a,b) of Ref. [14]. Also

$$k_T = \omega/c_T\ ; \quad c_T^2 = \mu/\rho\ . \qquad (3.4\ ,b)$$

The displacement discontinuity across the crack faces may be written as

$$[u_i](y) = \int_a^y d_i(s)ds\ ; \qquad i = x,y\ . \qquad (3.5)$$

Once $[u_i](y)$ has been computed, the radiated elastodynamic field can be computed by the use of an elastodynamic representation integral.

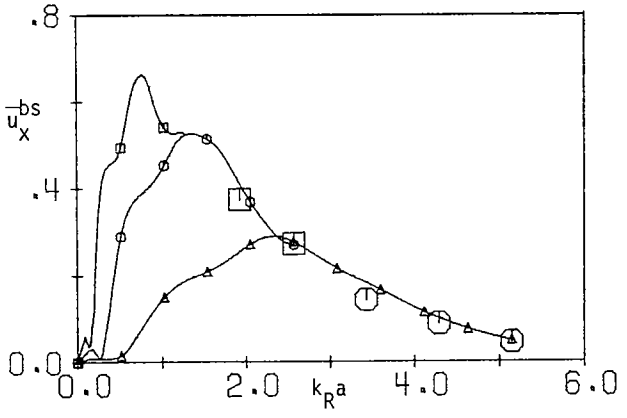

Fig. 11 Horizontal surface displacement in the back-scattered Rayleigh wave vs. $k_R a$, $\bar{u}^{bs}_x = |\, u^{bs}_x / u^{inc}_x\, |$, a/b = .1, a/b = .2, a/b = .4.

For three values of a/b the amplitudes of the horizontal displacement components of the back-scattered and forward-scattered surface waves, are shown in Figs.11 and 12, respectively. The amplitudes are plotted as functions of $k_R a = 2\pi a/\Lambda_R$, where Λ_R is the wavelength of the incident surface wave. It is noted that the amplitudes eventually decrease as $k_R a$ increases, i.e., as the wavelength becomes smaller relative to the distance from the nearest crack tip to the free surface. The reason for the decrease in amplitude is related to the exponential decay of surface waves with depth. A surface wave does not penetrate much deeper into a half-space than approximately one wavelength. Thus as the wavelength decreases the incident wave experiences less scattering by the sub-surface crack. For small enough wavelength the incident wave passes almost unhindered through the gap between the crack tip at y = a and the free surface. Figures 11 and 12 may be contrasted with the corresponding ones for a surface-breaking crack of depth d which have been presented in Ref.[11]. Very short waves are scattered strongly by a surface-breaking crack, and the amplitude spectra for both the forward-scattered and the back-scattered wave show an oscillation about a finite limit as $k_R d$ increases, where the period of the oscillation is directly related to the depth of the crack.

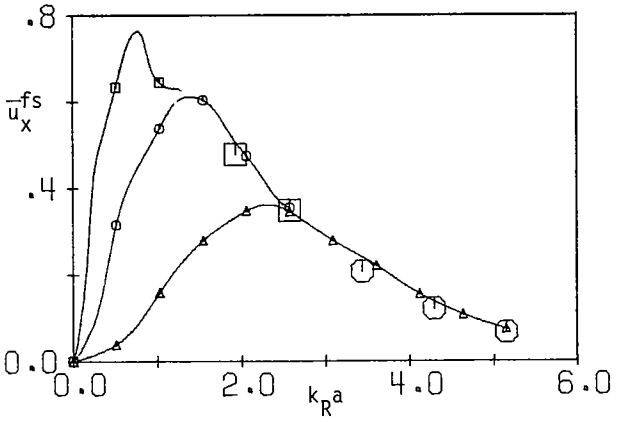

Fig. 12 Horizontal surface displacement in the forward scattered Rayleigh wave vs. $k_R a$,

$\bar{u}^{fs} = |u_x^{fs} / u_x^{inc}|$, ⊟ a/b = .1, ⊖ a/b = .2, △ a/b = .4.

The amplitudes of the scattered waves are also small when $k_R(b-a) \ll 1$, i.e., when $\Lambda_R \gg (b-a)$, in the long wavelength limit. It appears that for long wavelengths the scattering by a sub-surface crack and a surface-breaking crack are quite similar. A transition, characterized by a maximum in Figs. 11 and 12 occurs when the wavelength Λ_R is of the order (b-a). Thus, there is an optimum wavelength for a maximum scattering effect, at which the crack can easiest be detected by ultrasonic surface wave methods.

The cost of calculating these results is a function of $k_R(b-a)$ so it has not been possible to obtain the full curves over the whole range. However it is expected that when $k_R b$ is sufficiently large the scattering from the subsurface crack is approximately that due to a semi-infinite slit (i.e., the case when b/a = ∞). The curves are therefore expected to coincide with each other for sufficiently short wavelengths, and to verify this five additional points were obtained and are plotted as the large symbols in Figs. 11-13.

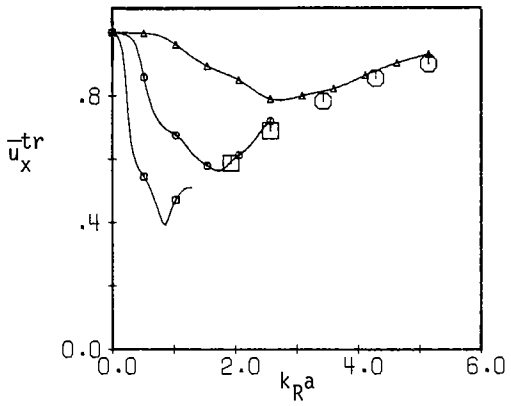

Fig. 13 Horizontal surface displacement in the transmitted Rayleigh wave vs. $k_R a$,

$\bar{u}_x^{tr} = |u_x^{tr} / u_x^{inc}|$, ⊟ a/b = .1, ⊖ a/b = .2, △ a/b = .4.

In experiments it is usually attempted to measure the backscattered wave and the forward-transmitted wave, where the latter is the sum of the incident wave and the forward-scattered wave, in the usual way. The amplitude of u_x for the forward transmitted wave is shown in Fig. 13. Consistently with the previous discussion the forward transmitted amplitude first decreases and then increases with increasing $k_R a$, and it approaches the amplitude of the incident wave for sufficiently large $k_R a$.

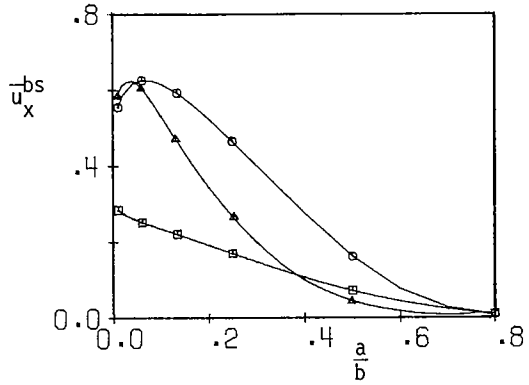

Fig. 14 Horizontal surface displacement in the back-scattered Rayleigh wave vs. a/b,

$\bar{u}_x^{bs} = |u_x^{bs}/u_x^{inc}|$, ⊟ $\frac{\omega b}{c_L} = 1$, ⊖ $\frac{\omega b}{c_L} = 3$, △ $\frac{\omega b}{c_L} = 5$.

Figure 14 shows the amplitude of the back-scattered wave as a function of a/b, for specific values of $k_R b$. An increasing value of a/b means in effect a smaller crack, since the crack length is proportional to 1-a/b, and hence a smaller back-scattered wave.

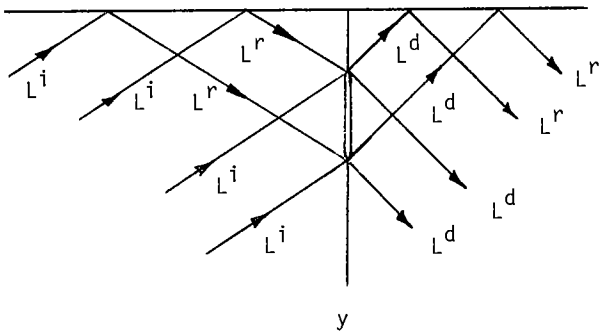

Fig. 15 Ray paths for incident L-rays.

3.2 Ray analysis of body-wave interaction with a sub-surface crack. Three ray paths are shown in Fig. 15. In the terminology of Section 2.4 these ray paths are L^iL^d, $L^iL^rL^d$, and $L^iL^dL^r$. In all three cases the ray paths can be either via the upper or via the lower crack tip. The interference of the time-harmonic signals carried by these ray paths is shown in Fig. 16. The interference of the two L^iL^d paths shows a simple structure of periodic peaks.

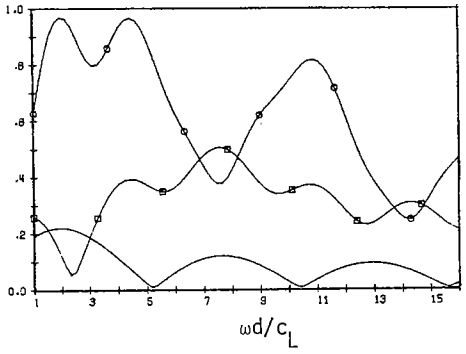

Fig. 16 Amplitudes of diffracted L-waves

—— $L^iL^d + L^iL^d$

—⊟— $L^iL^d + L^iL^d + L^iL^rL^d + L^iL^rL^d$

—⊖— $L^iL^d+L^iL^d+L^iL^rL^d+L^iL^rL^d+L^iL^dL^r+L^iL^dL^r$

ACKNOWLEDGEMENT

This work was carried out in the course of research sponsored by the Center for Advanced NDE operated by the Science Center, Rockwell International for the Advanced Research Project Agency and the Air Force Materials Laboratory under Contract F33615-80-C-5004.

REFERENCES

1. Achenbach,J.D., and Gautesen,A.K., "Geometrical Theory of Diffraction for Three-D Elastodynamics," J. Acoust. Soc. Amer., 61, 1977, pp. 413-421.
2. Achenbach, J.D., Gautesen, A.K., and McMaken,H., "Diffraction of Elastic Waves by Cracks - Analytical Results," in Elastic Waves and Non-Destructive Testing of Materials, edited by Y.H. Pao, AMD-Vol. 29, American Society of Mechanical Engineers, New York, 1978.
3. Achenbach, J.D., Gautesen, A.K. and McMaken,H., "Application of Geometrical Diffraction Theory to QNDE Analysis," ARPA/AFML Review of Progress in Quantitative NDE, edited by D.O. Thompson, Science Center, Rockwell International, Thousand Oaks, Cal., January 1979, pp. 321-330.
4. Achenbach,J.D., Gautesen, A.K. and McMaken,H., "Application of Ray Theory to Diffraction of Elastic Waves by Cracks," in Recent Developments in Classical Wave Scattering: Focus on the T-Matrix Approach, edited by V.K. Varadan and V.V. Varadan, Pergamon Press, 1980.
5. Achenbach,J.D., Gautesen,A.K., and McMaken,H., "Application of Elastodynamic Ray Theory to Diffraction by Cracks," Modern Problems in Elastic Wave Propagation, edited by J. Miklowitz and J. D. Achenbach, Wiley-Interscience, New York, 1978.
6. Achenbach,J.D., Adler, L., Lewis, D. Kent, and McMaken, H., "Diffraction of Ultrasonic Waves by Penny-Shaped Cracks in Metals: Theory and Experiment," J. Acoust. Soc. Am., 66, p. 1848, 1979.
7. Stone,S.F., Ghosh,M.L. and Mal,A.K., "Diffraction of Anti-Plane Shear Waves by an Edge Crack," J.Appl. Mech. 47, pp. 359-362, 1980.
8. Datta,S.K., "Diffraction of SH Waves by an Edge Crack," J. Appl. Mech.46, pp. 101-106, 1979.
9. Bowman,J.J., Senior,T.B.A., and Uslenghi,P.L.E., Electromagnetic and Acoustic Scattering by Simple Shapes, North-Holland, 1969.
10. Achenbach,J.D., Keer, L.M., and Mendelsohn, D.A., "Elastodynamic Analysis of an Edge Crack," J. Applied Mechanics, in press.
11. Mendelsohn,D.A., Achenbach,J.D., and Keer,L.M., "Scattering of Elastic Waves by a Surface-Breaking Crack, WAVE MOTION, in press.
12. Achenbach,J.D., Gautesen,A.K., and Mendelsohn, D.A., "Ray Analysis of Surface-Wave Interaction with an Edge Crack, IEEE Transactions Sonics and Ultrasonics, Vol. SU-27, pp. 124-129, 1980.
13. Achenbach, J.D., and Norris,A., "Interference of Corner-Reflected and Edge-Diffracted Waves for Scattering of Body-Waves by a Surface-Breaking Crack," submitted for publication.
14. Achenbach,J.D. and Brind, R.J., "Scattering of Surface Waves by a Sub-Surface Crack," submitted for publication.

Bernie Tittmann, Chairman (Rockwell Science Center): We have time for two questions.

Don Thompson (Ames Laboratory): Have you looked at the frequency composition of the scattered waves as they travel over the various paths? Presumably the subsurface crack would serve as a filter.

J.D. Achenbach (Northwestern University): The frequency composition? What you are referring to is an experimental pulse and what we are showing here is for a fast Fourier transform of such a pulse. These pictures are for harmonic waves.

Don Thompson: They are that, but would you expect there to be a difference if you started with different pulses?

J.D. Achenbach: You have to work with very short pulses. The higher the frequency content the better results you get.

Don Thompson: The filter characteristics of the various cracks should show up in the comparisons.

J.D. Achenback: Yes. The difference is the form of the amplitude. One being an essentially horizontal ripple, the other being a strongly decaying curve with frequency.

Laszlo Adler (Ohio State University): Have you worked out incident shear waves?

J.D. Achenbach: I'm glad you brought that up, because what we have done here are all first arrival longitudinal waves. Everything can be done equally well for shear waves. But as soon as you start talking about shear waves, you have to include all the preceding longitudinal waves.

Laszlo Adler: There is some indication you may have stronger signals with incident shear waves.

J.D. Achenbach: Definitely, for an incident shear wave, there is an indication that you have stronger signals. Unfortunately, incident shear waves still produces longitudinal waves.

Laszlo Adler: I notice you have a distribution of the input. Do you include finite transducer width?

J.D. Achenbach: Yes. And we integrate over the width of the transducer, quote-unquote transducer, which is just a width here of one inch, I think, or one centimeter.

Laszlo Adler: Not uniform but weighted integration.

J.D. Achenbach: Yes

Bernie Tittmann, Chairman: I just wanted to make a comment that the crack tip when radiated by surface waves radiates bulk waves.

J.D. Achenback: In the present paper we talked about the ray model for back scattering surface waves, and we didn't look into the medium itself, into the bulk waves generated by the surface waves, we can use the ray model for bulk waves as well.

Bernie Tittmann, Chairman: Thank you. We must move on.